Rational design of a synthetic farnesyl-electrostatic switch based on the hypervariable region of K-Ras4b

Allen K. Kim[1,2,3,*], Takanari Inoue[1,2,3,*]

[1]Department of Biomedical Engineering, Johns Hopkins University, School of Medicine, Baltimore, Maryland, United States.

[2]Department of Cell Biology, Johns Hopkins University, School of Medicine, Baltimore, Maryland, United States.

[3]Center for Cell Dynamics, Johns Hopkins University, School of Medicine, Baltimore, Maryland, United States.

[*]Correspondence to akim85@jhmi.edu, and jctinoue@jhmi.edu

Abstract

We rationally designed and developed a farnesyl-electrostatic switch that synthetically responds to an intended stimulus. Our design is a *de novo* amino acid sequence that mimics the switching behavior observed in K-Ras4b upon phosphorylation of serine-181. We built our peptide based on observations that the hypervariable region in the C-terminus of K-Ras4b contains: 1) a cluster of basic residues which electrostatically interact with the inner leaflet of the plasma membrane, 2) phosphorylation sites which will post-translationally change the positive charge content of the signaling sequence, and 3) a farnesylation recognition sequence which allows the protein to be anchored onto the cellular membrane system. We used this peptide to perform basic characterization of the farnesyl-electrostatic switch mechanism. We envision that it can have utility in future studies as a kinase sensor or as a module for perturbing signal transduction pathways.

Introduction

Dramatic shift in protein localization can be induced by post-translational modifications at localization sequences. In the case of K-Ras4b, the localization sequence is found in the C-terminus where the combination of polybasic residues and the -CAAX motif (where C is cysteine, A is aliphatic residue, and X is any residue) targets the protein to the plasma membrane. The -CAAX motif serves as a signal for enzymatic processing (involving farnesyltransferase, Ras-converting enzyme I, and isoprenylcysteine carboxyl methyltransferase) that leads to the attachment of a farnesyl group [1–3]. As farnesylation alone is not sufficient for plasma membrane targeting, many plasma-membrane-targeted farnesylated proteins including K-Ras4b also require the presence of a cluster of positively charged residues near the -CAAX motif [4–9].

Studies have shown that Protein Kinase C phosphorylation of serine-181 leads to a disruption of K-Ras4b's localization at the plasma membrane [10,11]. Schmick, et al. has shown that the electrostatic interaction between the positively charged residues in the protein and the negatively charged lipids in the plasma membrane is responsible for biasing the trafficking of K-Ras4b to the plasma membrane [12]. Phosphorylation in this region removes this bias by disrupting the favorable electrostatic interaction (Fig. 1A), a mechanism known as the farnesyl-electrostatic switch.

Characterizing the farnesyl-electrostatic switch mechanism has technical limitations, as changing the positively charged residues of the C-terminus of K-Ras4b directly affects its phosphorylability. We have overcome this limitation by designing a farnesyl-electrostatic switch using a known substrate sequence of Protein Kinase A (PKA). Unlike Protein Kinase C which requires a cluster of positively charged residues for substrate recognition [13], PKA requires only two arginines [14,15]. This allowed us to modulate the positive charge content of the switch in a substantial manner, while preserving phosphorylability, allowing us to explore parameters of the farnesyl-electrostatic switch that was previously not possible.

Results

Current understanding suggests that the farnesyl-electrostatic switch can be distilled into the following three basic components (Fig. 1B): 1) series of positively charged-residues that will electrostatically interact with negatively charged lipids in the plasma membrane, 2) phosphorylation sites that will change positive charge content to regulate signaling, and 3) -CAAX motif that will serve as a recognition sequence for farnesylation. In this study, we utilize these principles observed in the C-terminus of K-Ras4b to design a farnesyl-electrostatic switch that responds to PKA activation.

In our design of the PKA farnesyl-electrostatic switch, we mimicked this general pattern that we observed in K-Ras4b. We utilized a short PKA substrate sequence, Kemptide (LRRASLG), to serve as a source of phosphoserine [14]. We flanked a single lysine with the two Kemptide sequences, and a single leucine was removed from the second Kemptide sequence to maintain a consecutive sequence of positively charged residues. We, then fused a farnesylation substrate recognition sequence (TKCVIM), previously demonstrated to be sufficient for farnesyltransferase processing [16,17]. This resulted in a peptide design (FES-PKA) that encompassed all the basic properties observed in the C-terminus of K-Ras4b necessary for the switching functionality (Fig. 1B).

We expressed FES-PKA fused to EYFP in HeLa cells and noticed an enrichment in the plasma membrane. Upon activation of PKA with a cocktail of 50 µM forskolin (FSK) and 100 µM 3-isobutyl-1-methylxanthine (IBMX), the fluorescent signal redistributed to favor the intracellular membranes (Figs. 1C, 1D). The effect was reversible with the treatment of a 40 µM H89, a PKA inhibitor. Quantification was performed as described in the Methods. Line-scans of the micrographs shows the appearance and disappearance of a plasma membrane fluorescent signal (Fig. 1E), demonstrating the electrostatic switch mechanism of FES-PKA.

We explored the parameter space of this design to determine how different variables would affect the FES-PKA's response and localization. We initially hypothesized that introducing more phosphorylation sites to the peptide can increase the dynamic range of the FES-PKA's response from PKA stimulation (Fig. 2A). To test this hypothesis, we generated a peptide with a single phosphorylation site (monovalent) and a peptide with three phosphorylation sites (trivalent).

When co-transfected in cells, the monovalent peptide was largely localized in the intracellular membranes, due to an insufficient positive charge content. The trivalent peptide was observed in the nucleus in soluble form, as it appeared that the Ran machinery was being outcompeted by the farnesyltransferase. Quantification showed minor response from the monovalent peptide after PKA activation (Figs. 2B, 2C). The trivalent peptide was not included in the quantification due to the observed defects in localization.

We hypothesized that increasing the number of lysines flanked by the two phosphoserines will lead to a diminished response from PKA activation due to the unfavorable positive-to-negative charge ratio. We generated two additional peptides that contained three-lysine and five-lysine linkers, respectively. An increase in the number of lysines led to a concomitant decrease in the response from PKA activation (Figs. 2D, 2E). We also confirmed that the FES-PKA translocation was due to phosphorylation and not due to perturbation of PKA activity by generating mutants which disrupted phosphorylation (Figs. 3A, 3B). Mutations of both serines to alanines yielded no response, while having both serines intact led to the most robust response. Having only one of the serines led to an intermediate response.

In our design, we identified two clusters of basic residues, labeled as PBR #1 and PBR #2 (Fig. 3C). Based on the observation that the two serines are flanking PBR #2, we hypothesized that PBR #2 would have a more prominent role as a plasma membrane targeting sequence than PBR #1. We tested this hypothesis by mutating all the positively charged in PBR #1 and PBR #2 to alanines, respectively. As the arginines in P-2 and P-3 position are necessary for substrate recognition by PKA [15,18], mutations of these residues to alanines disrupts the phosphorylability of the substrate. For this reason, the serines were mutated to alanines in this experiment. Cells were co-transfected with the mutated FES-PKA and a non-phosphorylable, non-mutated FES-PKA. Mutations in PBR #1 did not appear to disrupt the initial localization, while mutations in PBR #2 caused a substantial enrichment in the intracellular membranes (Fig. 3C). Pearson's correlation was calculated by comparing the unmutated peptide against the three variant peptides (Fig. 3D).

Finally, polybasic targeting sequences in farnesylated proteins can be disrupted with calcium influx [9,19–22]. This is thought to occur the through binding of calmodulin, independent of

phosphorylation. We performed a similar experiment as previous by treating the cells with 1 µM ionomycin under a condition where the extracellular medium contained 1.8 mM Ca^{2+} (Figs. 4A). The time-profile shows the translocation of FES-PKA that is unphosphorylable. Both mutants regardless of the presence of serines responded to the influx of Ca^{2+} (Fig. 4B). We also compared the response of FES-PKA to the signal change with AKAR3EV [23], a Förster resonance energy transfer (FRET) sensor for PKA activity, 10 minutes after stimulation (Figs. 4C, 4D).

Discussion

Our design confirmed some of the previously established observations of the C-terminus of K-Ras4b. The six lysines in the positions 175 to 180 is responsible for serving as the signaling sequence to target the protein to the plasma membrane. Previous studies had already established serine-181 as a phosphate acceptor for Protein Kinase C. Our study further suggested that having two phosphorylation sites leads to a substantially more robust response than a single phosphorylation site (Figs. 3A, 3B). Based on this line of argument, we believe that phosphorylation at serine-175 of K-Ras4b can lead to a more robust translocation of K-Ras4b and speculate that serine-175 is a phosphate acceptor for an unknown kinase. Under this hypothesis, serine-175 and serine-181 can effectively behave as a logical AND gate that would yield the most robust response when both sites are phosphorylated.

Both K-Ras4b and FES-PKA's interaction with the plasma membrane is mediated by the presence of negatively charged lipids, the depletion of which causes the protein's dissociation from the plasma membrane [6,9]. This demonstrates that the farnesyl-electrostatic switch is not driven solely by protein phosphorylation[6,9]. This is further complicated by the observation that PDEδ [24–26] and calmodulin [19–21,27] are known binding partners of K-Ras4b that facilitate trafficking. It is currently unknown what role these proteins may have in the mechanism of the farnesyl-electrostatic switch. Due to FES-PKA's substantial difference in sequence to the C-terminus of K-Ras4b, the peptide described here can be used as a reference to determine the extent of these proteins' roles in the switching mechanism, if any.

To summarize, we have rationally designed a farnesyl-electrostatic switch that responds to PKA activity inside cells. This design is based on basic principles observed in the C-terminus of K-Ras4b where the modulation of positive charges by phosphorylation is the underlying mechanism for translocation. Because of its concise sequence, we envision that it can have further utility in future studies as a kinase sensor or as a module for perturbing signal transduction pathways.

Materials and Methods

Cell Culture and Transfection

HeLa (CCL-2, ATCC, Manassas, VA) cells were routinely passaged and cultured in DMEM (10-013-CV, Corning, Corning, NY) supplemented with 10% FBS (F2442, Sigma, St. Louis, MO) and maintained at 37°C in 5% CO_2. For imaging experiments, cells were seeded at a 30-40% confluence on a #1 coverslip (48380-080, VWR, Radnor, PA) placed inside 6-wells (353046, Corning, Corning, NY). Cells were transfected next day with FugeneHD (E2311, Promega, Madison, WI) at a ratio of 1:1 according to manufacturer's protocol, and 50 ng of DNA was added dropwise into each well. Cells were serum-starved with DMEM (17-205-CV, Corning, Corning, NY) without phenol red and supplemented with 2 mM L-glutamine (25-005-CL, Corning, Corning, NY) morning of the following day. In the afternoon of the same day, cells were imaged by transferring the coverslip to an Attofluor cell chamber (A7816, Invitrogen, Carlsbad, CA).

Image Acquisition

Images were acquired on an inverted microscope (IX81, Olympus, Tokyo, Japan) with a heated chamber that maintained conditions of 37°C and 5% CO_2 (WELS, Tokai-Hit, Fujinomiya, Japan). Images were acquired for 15 minutes or 25 minutes, as noted, at 1-minute interval. After 5 minutes, cells were treated with either 50 µM forskolin (F6886, Sigma, St. Louis, MO) and 100 µM IBMX (I5879, Sigma, St. Louis, MO) cocktail or 1 µM ionomycin (I-6800, LC Laboratories, Woburn, MA), as noted. Images were acquired with CMOS camera (C11440, Hamamatsu Photonics, Hamamatsu, Japan) on a 60x oil objective (60x PlanApo N, Olympus, Tokyo, Japan). Microscope was controlled with MetaMorph (Molecular Devices, San Jose, CA) with motorized stage controller (MS-2000, ASI, Eugene, OR) and filter wheel controller (Lambda 10-3, Sutter Instrument, Novato, CA). The sample was illuminated with a LED light source (pE-300, CoolLED, Andover, UK). For FRET experiments, images were acquired by exciting with CFP and detecting in the YFP channel. All experiments shown in a given panel were performed together.

Image Analysis

The signal at the intracellular membranes was quantified by co-expressing in cells an endomembrane marker that consisted of a prenylation sequence with no basic residues. ImageJ (NIH, Bethseda, MD) was used to track a 15x15 pixel (4.66 pixel = 1 µm) square region that contained the greatest average fluorescence intensity of the endomembrane marker. For fluorescence quantification, the background was subtracted, and the response of the signal was calculated by taking the ratio of signal with the average of the pre-treatment signal at the region of interest determined with the endomembrane marker. For FRET quantification, the background was subtracted, and the YFP emission signal was divided by the CFP emission signal. The reported response is this quantity normalized by the average of the pre-treatment signal for the whole cell.

Colocalization Analysis

For colocalization analysis, the role of the two polybasic residues clusters were characterized by mutating the positively charged residues to alanines, respectively. Cells were co-transfected with the mutated peptide and an unmutated peptide, both unphosphorylable. The extent of the colocalization between the two peptides was analyzed by first calculating a 20x20 pixel median filtered image for each channel and respectively subtracting them from the original images. The two background-subtracted images were

correlated using Pearson's correlation. The average of these Pearson's correlation from 30 cells is shown in Fig. 3D.

Statistical Analysis

Paired Student's t-test was used to test for statistical significance in Fig. 1D. Unequal variance t-test was used to test for statistical significance in Figs. 2C, 2E, 3B, 3D, and 4B. For each analysis, sample size was 30 cells collected over 3 independent experiments (10 cells each). All error bars represent mean±SEM.

DNA Cloning

DNA constructs were cloned by inserting annealed oligonucleotides into EYFP-C1 (Takara Bio, Kusatsu, Japan) and mCherry-C1 (Takara Bio, Kusatsu, Japan) at the SacII and BamHI site. The forward sequences of the inserted oligonucleotides with the restriction sites are as follows:

DNA construct	**cDNA sequence**	**Amino acid sequence**
Endomembrane Marker	GGGCcagcagcagcagcagaccaagtgcgtgatcatgTAGG	QQQQQQTKCVIM
FES-PKA (Unmutated)	GGGCctgagaagagccagcctgggcaagagaagagccagcctgggcaccaagtgcgtgatcatgTAGG	LRRASLGKRRASLGTKCVIM
FES-PKA (Monovalent)	GGGCctgagaagagccagcctgggcaccaagtgcgtgatcatgTAGG	LRRASLGTKCVIM
FES-PKA (Trivalent)	GGGCctgagaagagccagcctgggcaagagaagagccagcctgggcaagagaagagccagcctgggcaccaagtgcgtgatcatgTAGG	LRRASLGKRRASLGKRRASLGTKCVIM
FES-PKA (3 lysines)	GGGCctgagaagagccagcctgggcaagaagaagagaagagccagcctgggcaccaagtgcgtgatcatgTAGG	LRRASLGKKKRRASLGTKCVIM
FES-PKA (5 lysines)	GGGCctgagaagagccagcctgggcaagaagaagaagaagagaagagccagcctgggcaccaagtgcgtgatcatgTAGG	LRRASLGKKKKKRRASLGTKCVIM
FES-PKA (A-A mutant)	GGGCctgagaagagccgccctgggcaagagaagagccgccctgggcaccaagtgcgtgatcatgTAGG	LRRAALGKRRAALGTKCVIM
FES-PKA (S-A mutant)	GGGCctgagaagagccagcctgggcaagagaagagccgccctgggcaccaagtgcgtgatcatgTAGG	LRRASLGKRRAALGTKCVIM
FES-PKA (A-S mutant)	GGGCctgagaagagccgccctgggcaagagaagagccagcctgggcaccaagtgcgtgatcatgTAGG	LRRAALGKRRASLGTKCVIM
FES-PKA (PBR #1 mutant)	GGGCctggccgccgccgccctgggcaagagaagagccgccctgggcaccaagtgcgtgatcatgTAGG	LAAAALGKRRAALGTKCVIM
FES-PKA (PBR #2 mutant)	GGGCctgagaagagccgccctgggcgccgccgccgccgccctgggcaccaagtgcgtgatcatgTAGG	LRRAALGAAAAALGTKCVIM

Acknowledgments

We would like to thank Dr. Hideaki Matsubayashi for discussions that served as a starting point for the project and Dr. Abhijit Deb Roy for reading over the manuscript. We would also like to thank Dr. Kazuhiro Aoki for providing the AKAR3EV construct. This study was supported by National Institute of Health R01 GM123130 and DARPA HR0011-16-C-0139 (to T.I.).

Author Contributions

T.I. and A.K. conceived and designed this study. A.K. conducted all experiments and analyses. A.K. wrote the manuscript with contributions from T.I.

Additional Information

The authors declare no competing interests.

References

1. Ahearn, I. M., Haigis, K., Bar-Sagi, D. & Philips, M. R. Regulating the regulator: post-translational modification of RAS. *Nat. Rev. Mol. Cell Biol.* **13**, 39–51 (2012).
2. Wright, L. P. & Philips, M. R. CAAX modification and membrane targeting of Ras. *J. Lipid Res.* **47**, 883–891 (2006).
3. Choy, E. *et al.* Endomembrane Trafficking of Ras. *Cell* **98**, 69–80 (1999).
4. Gomez, G. A. & Daniotti, J. L. Electrical properties of plasma membrane modulate subcellular distribution of K-Ras: Membrane targeting of K-Ras. *FEBS J.* **274**, 2210–2228 (2007).
5. Hancock, J. F., Paterson, H. & Marshall, C. J. A polybasic domain or palmitoylation is required in addition to the CAAX motif to localize p21ras to the plasma membrane. *Cell* **63**, 133–139 (1990).
6. Heo, W. D. *et al.* PI(3,4,5)P3 and PI(4,5)P2 Lipids Target Proteins with Polybasic Clusters to the Plasma Membrane. *Science* **314**, 1458–1461 (2006).
7. Leventis, R. & Silvius, J. R. Lipid-Binding Characteristics of the Polybasic Carboxy-Terminal Sequence of K- *ras* 4B †. *Biochemistry* **37**, 7640–7648 (1998).
8. Roy, M.-O., Leventis, R. & Silvius, J. R. Mutational and Biochemical Analysis of Plasma Membrane Targeting Mediated by the Farnesylated, Polybasic Carboxy Terminus of K-ras4B †. *Biochemistry* **39**, 8298–8307 (2000).
9. Yeung, T. *et al.* Membrane Phosphatidylserine Regulates Surface Charge and Protein Localization. *Science* **319**, 210–213 (2008).
10. Bivona, T. G. *et al.* PKC Regulates a Farnesyl-Electrostatic Switch on K-Ras that Promotes its Association with Bcl-Xl on Mitochondria and Induces Apoptosis. *Mol. Cell* **21**, 481–493 (2006).
11. Jang, H. *et al.* Mechanisms of Membrane Binding of Small GTPase K-Ras4B Farnesylated Hypervariable Region. *J. Biol. Chem.* **290**, 9465–9477 (2015).
12. Schmick, M. *et al.* KRas Localizes to the Plasma Membrane by Spatial Cycles of Solubilization, Trapping and Vesicular Transport. *Cell* **157**, 459–471 (2014).
13. Nishikawa, K., Toker, A., Johannes, F.-J., Songyang, Z. & Cantley, L. C. Determination of the Specific Substrate Sequence Motifs of Protein Kinase C Isozymes. *J. Biol. Chem.* **272**, 952–960 (1997).
14. Kemp, B. E., Graves, D. J., Benjamini, E. & Krebs, E. G. Role of multiple basic residues in determining the substrate specificity of cyclic AMP-dependent protein kinase. *J. Biol. Chem.* **252**, 4888–4894 (1977).
15. Hutti, J. E. *et al.* A rapid method for determining protein kinase phosphorylation specificity. *Nat. Methods* **1**, 27–29 (2004).

16. Hicks, K. A., Hartman, H. L. & Fierke, C. A. Upstream Polybasic Region in Peptides Enhances Dual Specificity for Prenylation by Both Farnesyltransferase and Geranylgeranyltransferase Type I. *Biochemistry* **44**, 15325–15333 (2005).
17. Zhang, F. L. *et al.* Characterization of Ha-Ras, N-Ras, Ki-Ras4A, and Ki-Ras4B as in Vitro Substrates for Farnesyl Protein Transferase and Geranylgeranyl Protein Transferase Type I. *J. Biol. Chem.* **272**, 10232–10239 (1997).
18. Kemp, B. E. & Pearson, R. B. Protein kinase recognition sequence motifs. *Trends Biochem. Sci.* **15**, 342–346 (1990).
19. Fivaz, M. Reversible intracellular translocation of KRas but not HRas in hippocampal neurons regulated by Ca2+/calmodulin. *J. Cell Biol.* **170**, 429–441 (2005).
20. Villalonga, P. *et al.* Calmodulin Binds to K-Ras, but Not to H- or N-Ras, and Modulates Its Downstream Signaling. *Mol. Cell. Biol.* **21**, 7345–7354 (2001).
21. Abraham, S. J., Nolet, R. P., Calvert, R. J., Anderson, L. M. & Gaponenko, V. The Hypervariable Region of K-Ras4B Is Responsible for Its Specific Interactions with Calmodulin. *Biochemistry* **48**, 7575–7583 (2009).
22. Sperlich, B., Kapoor, S., Waldmann, H., Winter, R. & Weise, K. Regulation of K-Ras4B Membrane Binding by Calmodulin. *Biophys. J.* **111**, 113–122 (2016).
23. Komatsu, N. *et al.* Development of an optimized backbone of FRET biosensors for kinases and GTPases. *Mol. Biol. Cell* **22**, 4647–4656 (2011).
24. Schmick, M. *et al.* KRas Localizes to the Plasma Membrane by Spatial Cycles of Solubilization, Trapping and Vesicular Transport. *Cell* **157**, 459–471 (2014).
25. Chandra, A. *et al.* The GDI-like solubilizing factor PDEδ sustains the spatial organization and signalling of Ras family proteins. *Nat. Cell Biol.* **14**, 148–158 (2012).
26. Zimmermann, G. *et al.* Small molecule inhibition of the KRAS–PDEδ interaction impairs oncogenic KRAS signalling. *Nature* **497**, 638–642 (2013).
27. Sidhu, R. S., Clough, R. R. & Bhullar, R. P. Ca2+/calmodulin binds and dissociates K-RasB from membrane. *Biochem. Biophys. Res. Commun.* **304**, 655–660 (2003).

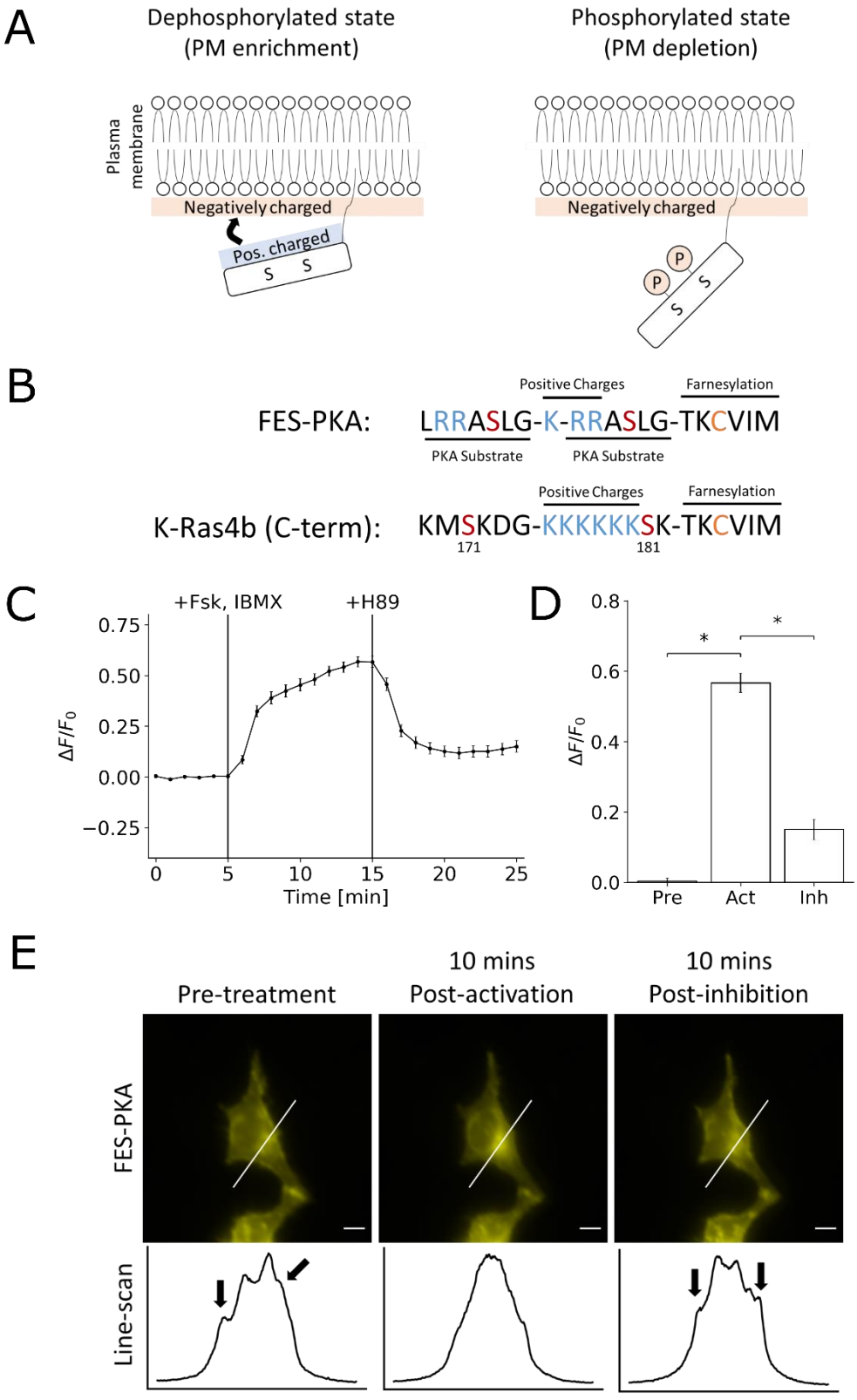

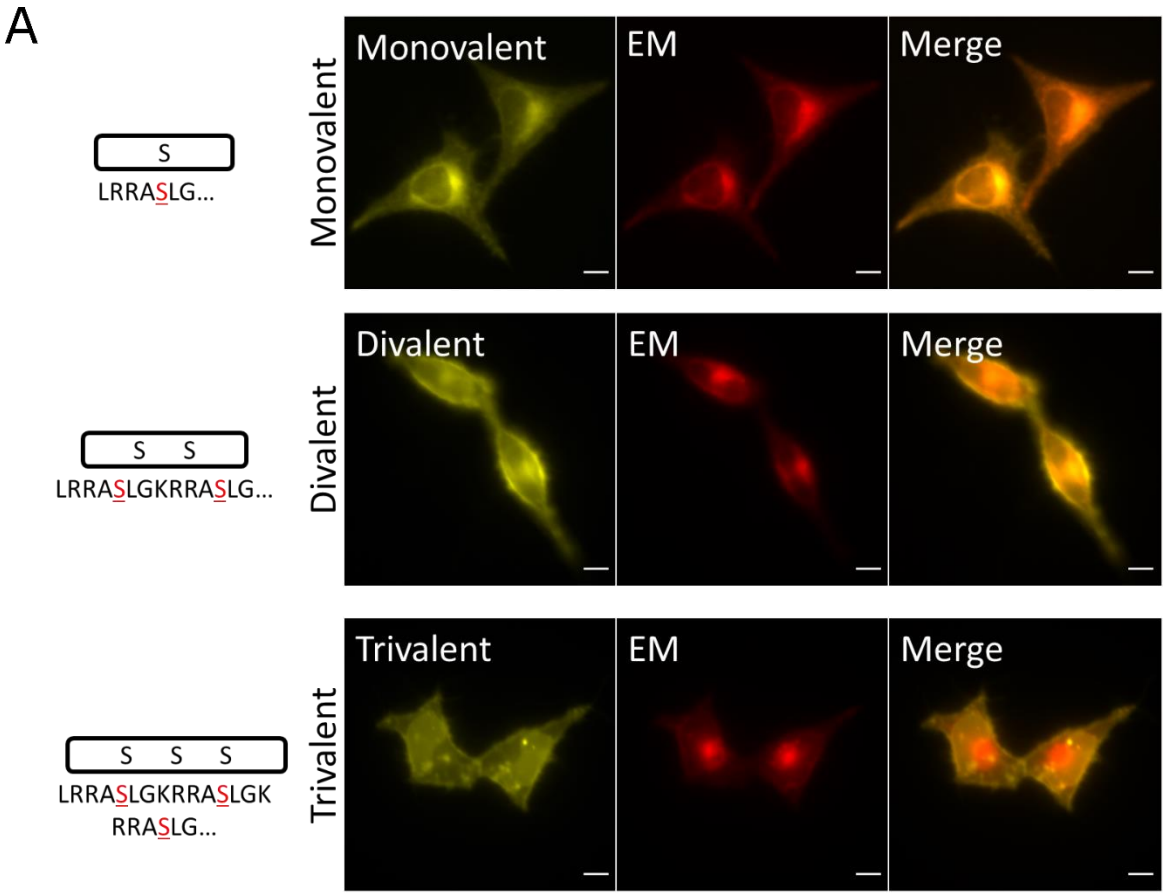

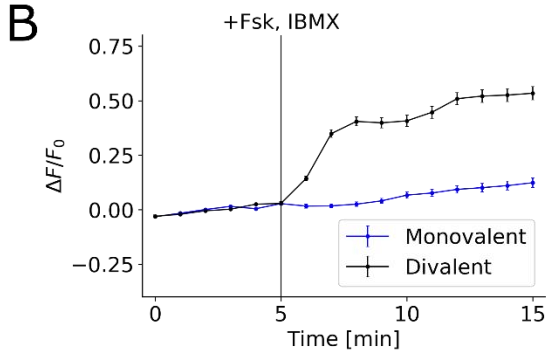

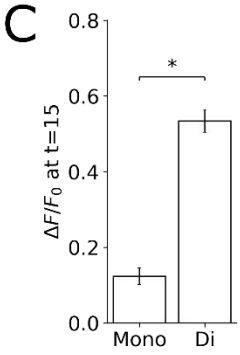

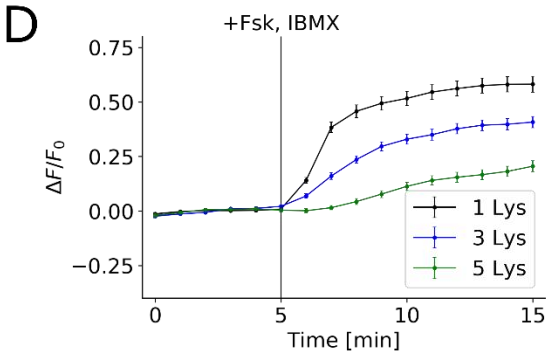

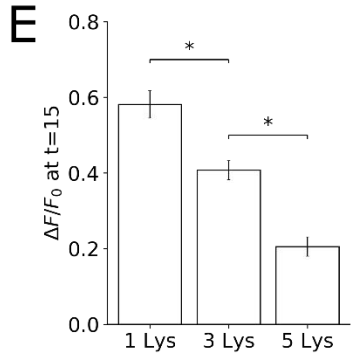

1

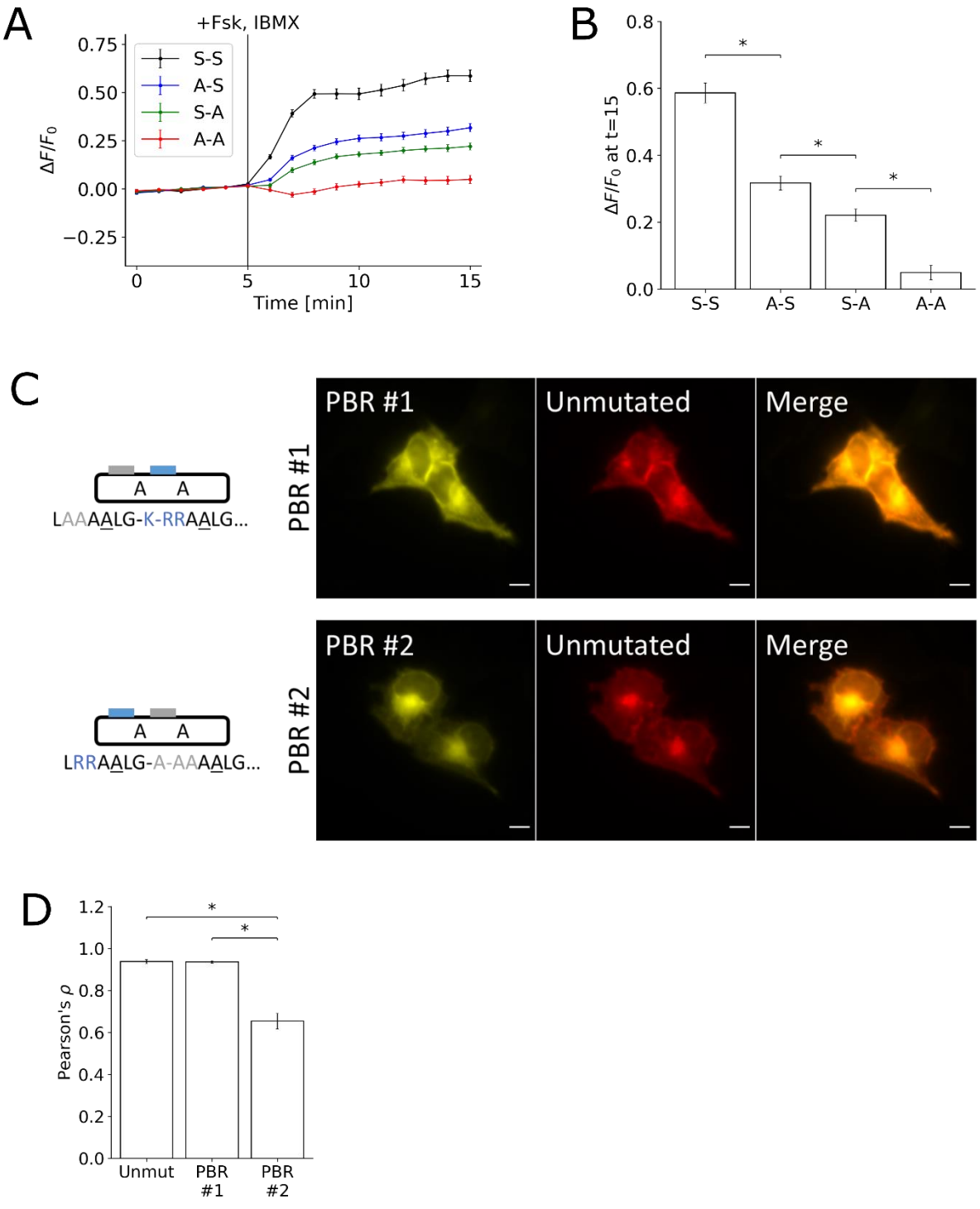

1

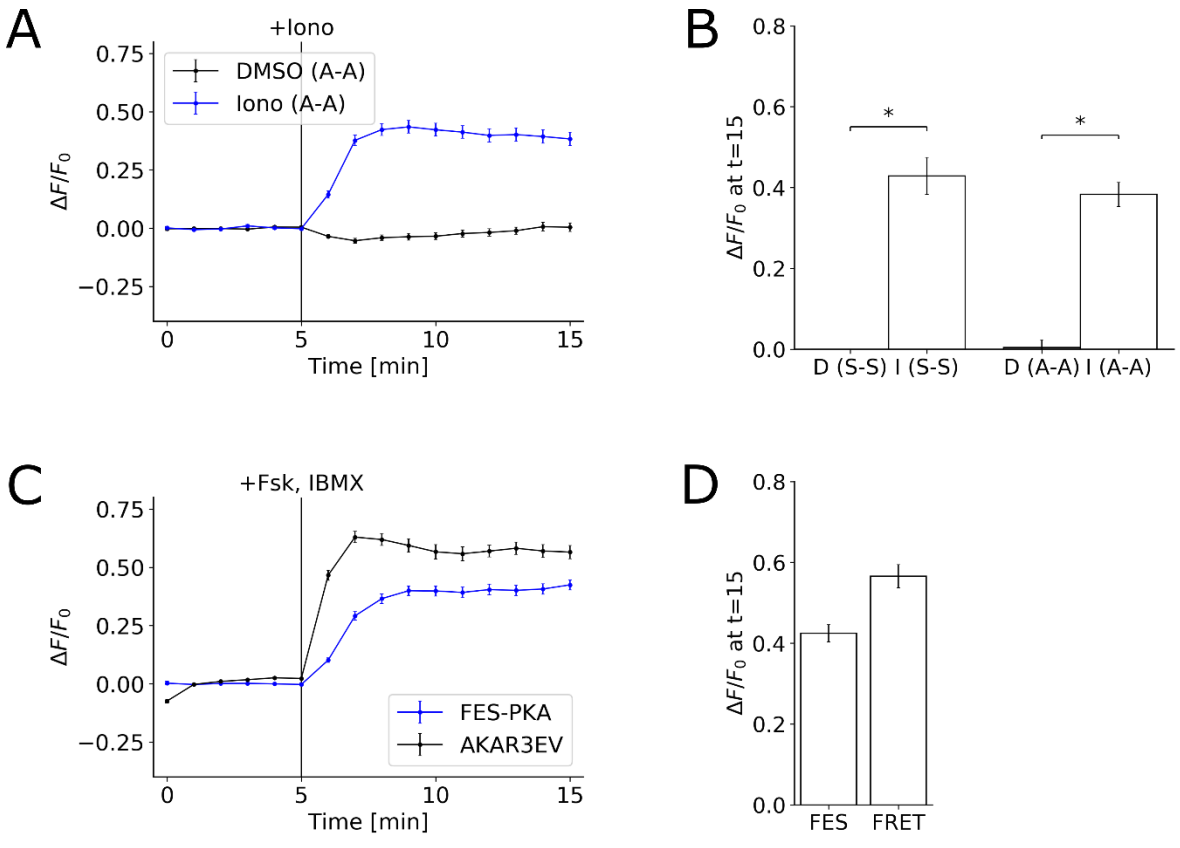

1

Figure 1: Basic Design of the Synthetic Farnesyl-Electrostatic Switch.

(A) Plasma membrane targeting of farnesylated proteins relies on the presence of positively charged residues near the C-terminus. The farnesyl-electrostatic switch relies on the regulation of this sequence through phosphorylation.

(B) C-terminus of K-Ras4b contains a cluster positive charges, two potential phosphate acceptors, and a farnesylation sequence, which was mimicked in the design for the FES-PKA.

(C) Time-profile shows the quantification of the fluorescent signal in response to PKA activation and reversal with PKA inhibition.

(D) Bar chart represents the signal change pre-treatment (at 5 minute), post-treatment with FSK+IBMX (at 15 minutes), and washout with H89 (at 25 min), respectively.

(E) Representative micrographs are shown of cells in the following states: pre-treatment, post-activation, and post-inhibition. Plots below the images show line-scans which reflect the signal intensity along the white line in the micrographs.

All data points in this figure represent an average signal intensity collected from 30 cells over 3 independent experiments (10 cells each), and error bars represents standard error of mean. * represents statistical significance: $p < 0.05$. Scale bar represents 10 µm.

Figure 2: Effects of Substrate Valency and Positive Charge Content on FES-PKA Localization and Response.

(A) Representative images are shown of cells co-transfected with peptides containing different number of substrates (monovalent, divalent, and trivalent) and an endomembrane (EM) marker. Divalent peptide is shown here as a reference and is the same amino sequence (FES-PKA) as shown in Fig. 1B.

(B) Time-profile shows quantification of fluorescent signal of monovalent and divalent peptides in response to PKA activation. Trivalent peptide was not included in quantification due to localization defects.

(C) Bar chart represents the signal change 10 minutes after PKA stimulation for the monovalent and divalent peptide.

(D) Time-profile shows quantification of fluorescent signal of increasing the positive charge content of the peptide.

(E) Bar chart represents the signal change 10 minutes after PKA stimulation for the three different lysine linkers.

All data points in this figure represent an average signal intensity collected from 30 cells over 3 independent experiments (10 cells each), and error bars represents standard error of mean. * represents statistical significance: $p < 0.05$. Scale bar represents 10 µm.

Figure 3: Role of Positively Charged Residues in Phosphorylation-Dependent Translocation.

(A) Time-profile shows quantification of peptides with various permutations of non-phosphorylable FES-PKA. In the notation S-S, the first letter represents whether the first phosphorylation site is mutated, and the second serine represents whether the second phosphorylation site is mutated.

(B) Bar chart represents the signal change for each of the mutations 10 minutes after PKA stimulation. **(C)** Micrograph represents cell images containing mutations disrupting the positively charged residues in the two clusters of basic residues, respectively.

(D) Bar chart represents the average Pearson's correlation calculated by comparing the three different peptides against their unmutated counterpart.
All data points in Figs. 2A and 2B represent data collected from 30 cells over 3 independent experiments (10 cells each), and error bars represents standard error of mean. * represents statistical significance: $p < 0.05$. Scale bar represents 10 µm.

Figure 4: Response of FES-PKA to Ca^{2+} Influx and Comparison of FES-PKA to AKAR3EV.
(A) Time-profile shows quantification of a non-phosphorylable FES-PKA in response to Ca^{2+} influx.
(B) Bar chart represents the signal change of a non-phosphorylable FES-PKA (A-A) and phosphorylable FES-PKA (S-S), respectively, after 10 minutes of treatment with DMSO (D) and ionomycin (I), respectively.
(C) Time-profile shows quantification of FES-PKA response in comparison to a PKA FRET sensor (AKAR3EV) in response to PKA activation.
(D) Bar chart represents the signal change for the FES-PKA (FES) and AKAR3EV (FRET) 10 minutes after PKA activation.
All data points represent an average signal intensity collected from 30 cells over 3 independent experiments (10 cells each), and error bars represents standard error of mean. * represents statistical significance: $p < 0.05$. Scale bar represents 10 µm.